

Macquarie University ResearchOnline

This is the published version of:

Peter Dekker, Helen M. Pask, David J. Spence, and James A. Piper, "Continuous-wave, intracavity doubled, self-Raman laser operation in Nd:GdVO₄ at 586.5 nm," *Opt. Express* **15**, 7038-7046 (2007).

Access to the published version:

<http://dx.doi.org/10.1364/OE.15.007038>

Copyright:

This paper was published in *Optics Express* and is made available as an electronic reprint with the permission of OSA. The paper can be found at the following URL on the OSA website: <http://www.opticsinfobase.org/abstract.cfm?URI=oe-15-11-7038>. Systematic or multiple reproduction or distribution to multiple locations via electronic or other means is prohibited and is subject to penalties under law.

Continuous-wave, intracavity doubled, self-Raman laser operation in Nd:GdVO₄ at 586.5 nm

Peter Dekker*, Helen M. Pask, David J. Spence and James A. Piper

Centre for Lasers and Applications, Macquarie University, NSW 2109 Australia

*Corresponding author: dekker@ics.mq.edu.au

Abstract: We report a continuous-wave self-Raman laser based on diode-pumped Nd:GdVO₄ giving first-Stokes output at 1173 nm and intracavity frequency-doubled output at 586.5 nm. A maximum cw output power at 1173 nm of 2 W was obtained for diode pump powers of 22 W and a maximum cw power at 586 nm of 678 mW with 16.3 W pump power. Infrared and yellow powers were limited by thermal lensing in the gain medium and parasitic oscillations of weak Nd³⁺ transitions. Quasi-cw operation at 50% duty-cycle reduced the thermal load in the laser/Raman crystal, allowing cavity stability to be obtained near maximum available pump power (25.7 W) for which the maximum quasi-cw yellow output power was 1.88 W.

©2007 Optical Society of America

OCIS codes: (140.3550) Lasers, Raman; (190.2620) Nonlinear optics, frequency conversion; (140.3380) Laser Materials.

References and links

1. T. T. Basiev and R. C. Powell, "Special issue on solid state Raman lasers - Introduction," *Opt. Mater.* **11**, 301-306 (1999).
2. H. M. Pask, "The design and operation of solid-state Raman lasers," *Prog. Quantum Electron.* **27**, 3-56 (2003).
3. R. P. Mildren, H. M. Pask, H. Ogilvy, and J. A. Piper, "Discretely tunable, all-solid-state laser in the green, yellow, and red," *Opt. Lett.* **30**, 1500-1502 (2005).
4. H. M. Pask, "Continuous-wave, all-solid-state, intracavity Raman laser," *Opt. Lett.* **30**, 2454-2456 (2005).
5. A. A. Demidovich, A. S. Grabtchikov, V. A. Lisinetskii, V. N. Burakevich, V. A. Orlovich and W. Kiefer, "Continuous-wave Raman generation in a diode-pumped Nd³⁺:KGd(WO₄)₂ laser," *Opt. Lett.* **30**, 1701-1703 (2005).
6. V. A. Orlovich, V. N. Burakevich, A. S. Grabtchikov, V. A. Lisinetskii, A. A. Demidovich, H. J. Eichler, and P. Y. Turpin, "Continuous-wave intracavity Raman generation in PbWO₄ crystal in the Nd:YVO₄ laser," *Laser Phys. Lett.* **3**, 71-74 (2006).
7. P. Dekker, H. M. Pask and J. A. Piper, All-Solid-State 704 mW continuous-wave yellow source based on an intracavity, frequency-doubled crystalline Raman laser, *Opt. Lett.* **32**, 1114-1117 (2007).
8. Y. F. Chen, "Efficient 1521-nm Nd:GdVO₄ Raman laser," *Opt. Lett.* **29**, 2632-2634 (2004).
9. Y. F. Chen, "High-power diode-pumped actively Q-switched Nd:YVO₄ self-Raman laser: influence of dopant concentration," *Opt. Lett.* **29**, 1915-1917 (2004).
10. T. T. Basiev, S. V. Vassiliev, M. E. Doroshenko, V. V. Osiko, V. M. Puzikov and M. B. Kosmyna, "Laser and self-Raman-laser oscillations of PbMoO₄:Nd³⁺ crystal under laser diode pumping," *Opt. Lett.* **31**, 65-67 (2006).
11. T. Omatsu, Y. Ojima, H. M. Pask, J. A. Piper, and P. Dekker, "Efficient 1181 nm self-stimulating Raman output from transversely diode-pumped Nd³⁺:KGd(WO₄)₂ laser," *Opt. Commun.* **232**, 327-331 (2004).
12. N. S. Ustimenko and E. M. Zabolotn, "A small Raman laser based on a KGd(WO₄)₂:Nd³⁺ crystal ($\lambda=1.538$ μm) with passive resonator Q switching," *Instrum. Exp. Tech.* **48**, 239-240 (2005).
13. A. A. Kaminskii, S. N. Bagayev, K. Oka, H. Shibata, K. Ueda, K. Takaichi, H. J. Eichler, and H. Rhee, "Observation of stimulated Raman scattering in the tetragonal crystal YbVO₄," *Laser Phys. Lett.* **3**, 263-267 (2006).
14. J. T. Murray, W. L. Austin, and R. C. Powell, "Intracavity Raman conversion and Raman beam cleanup," *Opt. Mater.* **11**, 353-371 (1999).
15. M. E. Innocenzi, H. T. Yura, C. L. Fincher and R. A. Fields, "Thermal modeling of continuous-wave end-pumped solid-state lasers," *Appl. Phys. Lett.* **56**, 1831-3 (1990).

16. Laser cavity analysis and design, (LAS-CAD), GmbH Germany, www.las-cad.com.
 17. J. L. Blows, T. Omatsu, J. Dawes, H. Pask, and M. Tateda, "Heat generation in Nd:YVO₄ with and without laser action," *IEEE Photon. Technol. Lett.* **10** 1727-1729 (1998)
-

1. Introduction

Raman lasers which employ intracavity Raman shifting in crystalline materials are widely recognized as a highly efficient and practical means of extending the spectral coverage of established Neodymium based laser systems [1, 2]. The visible spectrum, the yellow-orange region in particular, can be efficiently accessed through intracavity frequency doubling of the Stokes field [3]. These systems are simple and versatile, and by choosing different laser and Raman crystals, a range of output wavelengths can be obtained for potential applications in the areas of medicine, biomedicine and remote sensing. Prior to 2004, all reported crystalline Raman lasers were pulsed devices. However in the past 2 years, diode-pumped cw intracavity Raman laser action has been achieved [4-6] through careful attention to resonator design, including the minimization of resonator losses. Most recently, we have reported [7] intracavity doubling (in LBO) of an intracavity Raman laser based on a Nd:GdVO₄ laser crystal and a KGd(WO₄)₂ Raman crystal, from which 704 mW cw output was obtained at 588 nm with an overall diode to yellow conversion efficiency of 5.1%. The most critical design parameters for such a yellow laser source are thermal lens management, optimizing the mode size in each of the three crystals and minimizing resonator losses.

A subgroup of intracavity Raman lasers are the self-Raman lasers, in which the laser crystal is also Raman-active. Self-Raman laser action in Q-switched devices has been investigated for a variety of media, of which the most promising are Nd:GdVO₄ [8], Nd:YVO₄ [9], Nd:PbMoO₄ [10] and Nd:KGd(WO₄)₂ [11, 12]. By eliminating the need for a separate Raman crystal, self-Raman lasers can have important benefits of lower resonator losses and shorter resonators, and these were critical factors in the first demonstration of a diode-pumped cw self-Raman laser by Demidovich [5] who obtained cw operation of a self-Raman Nd:KGW laser giving first-Stokes output powers of 54 mW for a 1.5 W diode-pump.

There are two significant drawbacks associated with self-Raman lasers however: first, thermal loading of the laser/Raman crystal is exacerbated by the additional thermal loading from the Raman conversion process; and second, there is no flexibility to separately optimize the mode sizes in the laser and Raman crystals as may be required for best efficiency. Choice of self-Raman material is therefore very important – the crystal needs to have good thermal properties as well as a high Raman gain. Of the self-Raman materials reported to date, Nd:GdVO₄ and Nd:YVO₄ are widely available, have good thermal properties, and a moderately high Raman gain coefficient of around 4.5cm/GW [13].

In this paper we report intracavity-doubled cw self-Raman laser operation based on diode-pumped Nd:GdVO₄ generating 678 mW in the yellow at 586 nm (with a diode-to yellow conversion efficiency of 4.2%) and 2 W cw at the first-Stokes at 1173 nm. Maximum cw powers at both wavelengths were limited by the effects of strong thermal lensing in the laser/Raman crystal. To explore the potential for generating higher cw powers, the laser was operated in quasi-cw mode (50% pump duty-cycle) to reduce the thermal loading of the crystal, whereupon we obtained a maximum instantaneous output power of 1.88 W (940 mW average) at 586 nm. To the best of our knowledge this is the first report of cw self-Raman laser operation in Nd:GdVO₄ and efficient intracavity doubling of the first-Stokes field to the visible, and the highest output power of any self-Raman laser.

2. Set-up

The Raman laser configuration is illustrated in Fig. 1. The resonator was bounded by a flat input mirror (coated 96%T at 808 nm, HR (0.006%T) at 1063 nm, 0.004%T at 1173 nm and 93%T at 586 nm) and for infrared (first-Stokes) operation, a 250 mm Roc concave output mirror (coated 0.09%T at 1063 nm, and 0.4%T at 1173 nm). For intracavity frequency-

doubled operation the output mirror was a 200 mm Roc concave mirror coated identically to the input mirror.

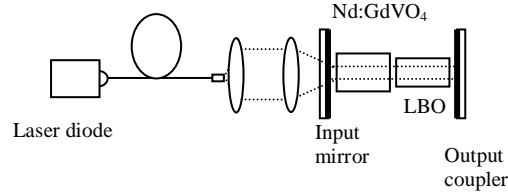


Fig. 1. Schematic of self-Raman laser including an optional LBO crystal for generating yellow emission.

The pump source was a 30 W fiber-coupled 808 nm diode laser ($\phi=400\ \mu\text{m}$, $\text{NA} \sim 0.22$), imaged with unity magnification through the input mirror onto the AR-coated (1064-1200 nm) a-cut 0.3at. % Nd:GdVO₄ crystal (3x3x10 mm). Second harmonic generation (SHG) of the 1173 nm first-Stokes line was obtained using a 3x3x10 mm non-critically phase-matched (NCPM, $\theta=90^\circ$, $\phi=0^\circ$) LBO crystal coated AR at 1064-1200 nm and temperature tuned to $\sim 45^\circ\text{C}$. Cavity lengths ranged from 13 to 24 mm (24 mm with the inclusion of LBO).

The thermal lens induced in the Nd:GdVO₄ crystal by pump and Raman heating has a strong influence on the cavity stability and the mode-size in the crystal, thus the cavity length was kept to a minimum determined by the length of the intracavity components. In experiments exploring high peak pump powers the thermal effects were reduced by modulating the diode pump beam with a mechanical chopper giving a 200 Hz pump train corresponding to a 50% duty-cycle.

Operation at the fundamental wavelength (1063 nm) of the Nd:GdVO₄ laser was characterized using a flat output mirror with 5% transmission (and of course with the LBO removed). For a cavity length of 45 mm a maximum of 14.4 W cw output was obtained at maximum pump power (26.3 W) incident on the laser crystal. Note that for cavity length 66 mm, the onset of cavity instability occurred at ~ 20 W pump power.

3. Self-Raman operation at the first stokes wavelength (1173 nm)

For operation at 1173 nm, we investigated laser performance for 2 cavity lengths: 13 and 24 mm. For the shortest physical cavity length possible (13 mm) with a 0.4%T (at 1173 nm) output coupler, threshold for lasing on the fundamental wavelength was reached at 0.7 W pump power while the threshold for cw Raman oscillation was 4.6 W pump power (see Fig. 2). Maximum cw output power obtained on the first-Stokes line at 1173 nm was 2.04 W at 22 W pump power, limited by the onset of optical damage to the crystal coatings (rather than the effects of thermal lensing for this shortest of cavities). We believe that the observed optical damage was primarily due to the high circulating powers in the absence of substantial output coupling.

For the 24 mm-long cavity, the first-Stokes output power reached a maximum of 1.1 W at 18 W pump power but declined at higher pump powers with the onset of cavity instability. Based on this observation we estimate the thermal lens in the Nd:GdVO₄ crystal was approximately 17 mm (taking account of the refractive index of the crystal itself).

Maximum residual 1063 nm powers, ie the 1063 nm output 'leaking' through the end mirror, was ~ 1.8 W indicating that the output coupling coating was by no way optimized. Substantial increases in Raman power can be expected by increasing the cavity-Q at the fundamental while simultaneously increasing the Raman output coupling to the order of 2-3%. As the noncoupling losses at the Raman wavelength are estimated to be of the order of 1% we are optimistic Raman output powers as high as 4 W could be reached through optimization of the optical coating of the output coupler and yet higher output powers by better thermal lens management.

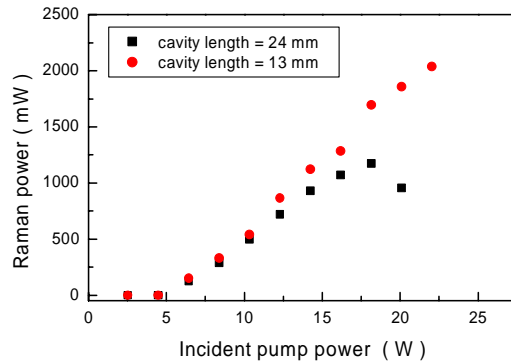


Fig. 2. Cw Raman (1173 nm) output powers as a function of incident pump power for 13 and 24 mm physical cavity lengths.

The spectral characteristics of the fundamental and Stokes output were investigated using an optical spectrum analyzer with 0.06 nm resolution. The (time-averaged) fundamental spectrum was centered at 1063.2 nm with a bandwidth of 0.5-0.8 nm. Typically the output bandwidth increased with pump power and exhibited complex structure (discussed in the following section). The spectrum of the first-Stokes output was centered at 1173 nm, also with a bandwidth of approximately 0.5-0.8 nm. The Raman laser output was linearly polarized for all pump powers with polarization axis parallel to that of the fundamental laser at 1063 nm which itself was polarized parallel to the crystal c-axis (π -polarized).

Beam quality measurements of the 1173 nm first-Stokes laser output and also of the residual fundamental output showed that the M^2 -value varied both with pump power and on the level of depletion of the fundamental. Data from these experiments are shown in Fig. 3. For operation at the fundamental wavelength (with a 5% output coupler and SRS not occurring) the output at 1063 nm had a maximum M^2 -value of 8.3. For increased cavity-Q, corresponding to the Raman laser mirror set, the beam quality of the fundamental deteriorated rapidly after the onset of Raman oscillation, with the M^2 -value reaching as high as 14 at maximum pump/Raman power. However beam quality for the Raman output was much superior, the M^2 reaching a maximum value of only 3 at maximum pump/Raman power. This is a consequence of Raman beam clean-up as has been reported previously for pulsed Raman lasers [2, 14].

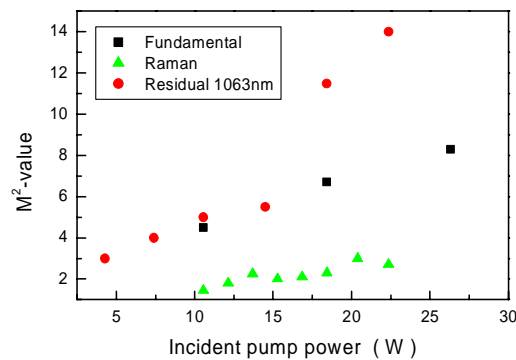


Fig. 3. Beam quality factor (M^2) of optimized fundamental, optimized Raman and residual fundamental in an optimized Raman configuration as a function of incident pump power.

The peak-to-peak amplitude noise at maximum pump power was measured to be approximately 5% ($2\sigma/\text{av}$) for frequencies <200 MHz, while the longer-term (10-minute) power stability was determined using a thermal power meter to be better than 3%.

4. Frequency-doubled operation in the visible (586 nm)

For studies of intracavity frequency-doubling of the Raman optical field the infrared output coupler was replaced with the yellow output coupler (highly reflective at both the fundamental and 1st-Stokes wavelengths) and the resonator was extended by 12 mm (to total length 24 mm) to accommodate the LBO frequency-doubling crystal. This extended resonator length necessarily lowered the maximum pump power for which resonator stability could be maintained. Despite the added losses arising from the insertion of the LBO crystal in the cavity, the substantially higher Q of the resonator for the infrared wavelengths, resulted in a reduction of pump power required to reach 1st-Stokes threshold to 2.4 W (*cf* 4.6 W for the Raman only optimized system).

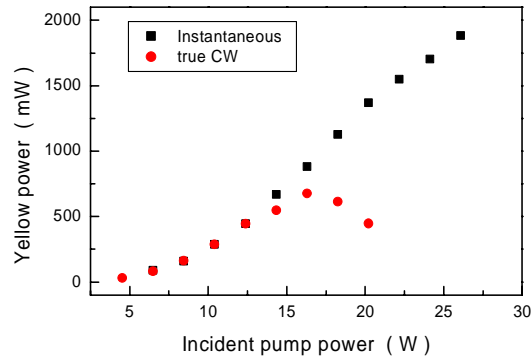


Fig. 4. Yellow power as a function of incident pump power in cw and quasi-cw operation.

The (single-ended) cw powers at 586 nm as a function of diode-pump power incident on the laser crystal are shown in Fig. 4. Maximum cw output powers at 586 nm of 678 mW were obtained with incident pump powers of 16.3 W. Residual fundamental and 1st-Stokes powers were each less than 200 and 50 mW respectively. We expect that similar powers (at 586 nm) were generated in the opposite direction to those measured and were either absorbed in the Nd:GdVO₄ laser crystal (the absorption coefficient at 586 nm was measured to be greater than 2 cm^{-1}) or lost through the input mirror. The maximum yellow power was limited by a combination of thermal lensing driving the cavity towards the boundary of resonator stability and the onset of a competing fundamental laser transition (with orthogonal polarization) near 1066 nm. Raman oscillation could not be obtained simultaneously with orthogonal polarization vectors and so operation on this transition acted as a source of loss for both the Raman and second harmonic output. Maximum diode-yellow optical conversion efficiency for fully cw operation was 4.2%, taking into account only the power measured beyond the output coupler. Taking account of the backward-propagating yellow beam, internal diode-yellow efficiency can be estimated to be $>8\%$.

Spectral characteristics of the fundamental and 1st-Stokes outputs are shown in Fig. 5 before and after the onset of the parasitic transition at 1066 nm (which occurs at approximately 20 W pump power). We believe simultaneous operation at 1063 and 1066 nm arises as the increasing loss for the 1063 nm line (as the Stokes power increases) results in an increased inversion in the crystal eventually allowing the slightly lower gain 1066 nm line to oscillate. Operation at 1066 nm could be prevented by adding some small polarization dependant loss as the two wavelengths are orthogonally polarized.

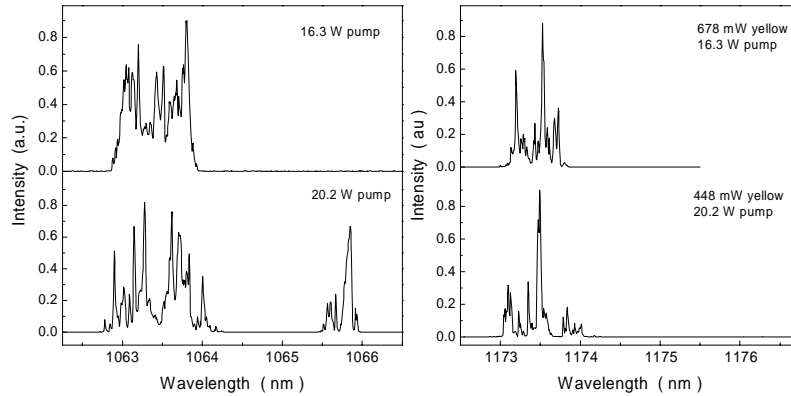


Fig. 5. Cw fundamental and Raman spectra at 16.3 W (maximum yellow output power) and 20.2 W pump power.

To explore the potential for generating higher cw yellow output powers at higher pump powers (above 17 W) we undertook experiments in which the diode pump was operated at reduced duty cycle (50% at 200 Hz repetition rate) using a mechanical chopper inserted in close proximity to the optical fibre pump. The rise time (10-90%) of the pump was less than 10% of the pump pulse length (2.5 ms). The fundamental laser threshold however was reached well before the pump reached its maximum, typically within 25 μ s and Raman oscillation 3 μ s later resulting in a square wave quasi-cw pulse train. There was no measurable difference in threshold pump powers for the cw and quasi-cw cases. The relatively slow turn on of the pump prevented significant relaxation oscillation spiking that would otherwise have resulted in damaged coatings in the high-Q resonator. The reduced thermal load in the laser crystal in this quasi-cw mode of operation permitted instantaneous pump powers up to the maximum available without any roll-over in output power (nor any evidence of lasing on the parasitic 1066 nm transition). Data for operation in this quasi-cw mode is included in Fig 4: we obtained maximum (single-ended) yellow output power of 1.88 W (940 mW average) for instantaneous diode pump powers of 26 W (13 W average) with a corresponding diode-to-yellow conversion efficiency of 7.2%. For pumping at 50% duty cycle the average output power in the yellow was stable over a much larger range of diode powers, consistent with our premise that thermal lensing and associated variations of spatial mode distribution was the primary factor causing the output power roll-over. The substantially improved powers and efficiencies achieved for operation with lower thermal loading of the laser/Raman crystal indicate that significantly higher cw output powers can be achieved with further attention to thermal management for the crystal and related optimization of resonator design.

For both cw and quasi-cw modes of operation the beam quality of the yellow emission was dominated by the aberrations induced by the strong thermal lens as well as the large number of transverse modes that reached threshold in the high-Q cavity. At low output powers (\sim 150 mW at 586 nm in quasi-cw operation) we obtained Gaussian-like output with M^2 -values of between 2 to 3. At near maximum output power the spatial mode was strongly peaked with a corresponding higher M^2 -value of between 5 and 6. Beam profiles and x-y intensity curves near threshold and at maximum pump power are shown in Figs. 6(a) and 6(b). The reduced beam quality of the yellow emission compared with the Raman only output is predominately attributed to the increased number of transverse modes that were able to oscillate in the substantially higher Q cavity used for operation at 586 nm.

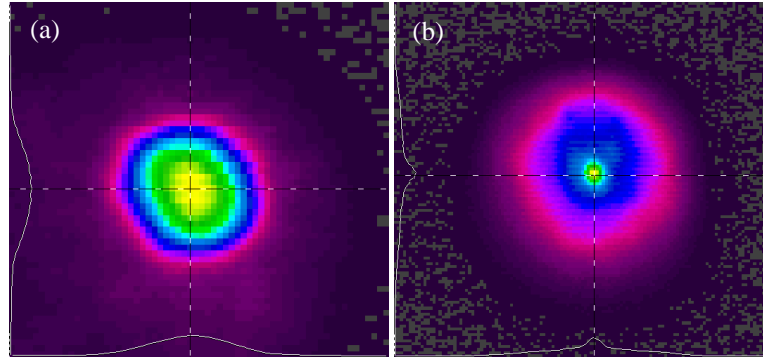


Fig. 6. (a). Near field beam profiles of quasi-cw yellow emission, with near 150 mW output [with x 2 magnification c.f Fig. 6(b)] and (b) near maximum pump with 1.88 W output.

The amplitude stability of the yellow emission (cw and quasi-cw) was dominated by the noise from competing transverse modes. In true cw operation using a photodiode with a 5 ns response time we measured the amplitude stability to be 15% ($2\sigma/av$). The long-term noise measured over a 10 minute period (that measured with a thermal power detector) was however only 5.7%. These figures were much improved in the quasi-cw case with a short-term noise value of 8.6% and a variation in average power of only 1.8%. Further improvements are expected by stabilizing the transverse mode structure.

5. Discussion of thermal loading

On the basis of the preceding experimental results, we note that thermal lensing is the main factor limiting further power scaling of the yellow output. Experimentally we observe (for a fixed cavity length of 24 mm) different output power characteristics resulting from the different thermal loads for systems operating at the fundamental, first Stokes and yellow wavelengths. These results are summarized in Fig. 7 and are discussed further below. It is certainly possible, though challenging, to design a resonator which accommodates the strong thermal lens. However it is also important to consider and understand the origin of the thermal loading which results in the strong thermal lens. For the case of first Stokes operation thermal loading arises from the absorption of pump light and through the inelastic nature of the SRS process, while for yellow optimized operation an additional thermal load from absorption of the backward propagating yellow emission must also be taken into consideration.

The calculated contributions of each of these three thermal loading mechanisms are listed in Table 1 with approximate cumulated thermal lens values calculated for the case of 20 W pump power. The calculations were made following the approach of Innocenzi et al. [15]. We note that it is difficult to assess the relevant mode size for the different thermal loading processes as the exact waist position and effective mode size is not well known. For the diode-pump induced thermal load the pump spot size was geometrically averaged over the pump absorption length (~ 3 mm at 20 W of pump power). For the SRS and yellow absorption loading mechanisms the mode size used to calculate the thermal lens was obtained by averaging the calculated [16] fundamental-mode (TEM_{00}) size over the Nd:GdVO₄ crystal length (taking into account the generated thermal lens in a 24 mm resonator) and then multiplying by $\sqrt{M^2}$ -value and iterating this process until a self-consistent result was obtained. The thermal load factors were taken to be 0.32 for the pump loading [17], 0.1 for the SRS process and 0.95 for yellow light absorption (based on measured absorption coefficient of 2 cm^{-1} at 586 nm in Nd:GdVO₄ crystal). For first Stokes operation, we estimate (from resonator loss considerations) that the optical power generated was 6 W, of which 4 W was lost by internal losses.

Table 1. Calculations of induced thermal lensing by pump loading, SRS and yellow absorption, in NdGdVO₄ for the cases of fundamental operation, first Stokes operation and yellow operation with 20 W of diode pump power.

	<i>Thermal loading process</i>		
	Pump loading	SRS	Yellow absorption
Wavelength	808 - 1063 nm	1063 – 1173 nm	586.5 nm
Thermal load factor	0.32	0.1	0.95
Optical power	20 W	6 W	0.7 W
Thermal load @ 20W pump	4.8 W	~0.6 W	0.67
TEM ₀₀ mode size	$\omega_{av}(\text{pump})=414 \mu\text{m}$	$M^2(1173)=3$ $\omega_{\text{TEM}00}=100 \mu\text{m}$ $\omega_{1173}=173 \mu\text{m}$	$M^2(586)=5$ $\omega_{\text{TEM}00}=88 \mu\text{m}$ $\omega_{586}=341 \mu\text{m}$
Predicted thermal lens power	19 diopters	10.4 diopters	8.5 diopters
	System optimized for:		
	Fundamental operation	First Stokes operation	Yellow operation
Cumulative thermal lens power	19 diopters	29.4 diopters	37.9 diopters
Cumulative lens focal length	5.2 cm	3.4 cm	2.6 cm

The calculations shown in Table 1 (based on 20 W diode pump powers incident on the laser crystal) indicate that the thermal lens taking only pump induced heating into account has a focal length of approximately 52 mm. This compares reasonably well with our earlier estimate of the thermal lens focal length (60 mm) for operation on the fundamental alone at 20 W pump power, and as expected, there is no rollover observed in the output power at the fundamental.

If we then take into account the additional thermal loading due to Raman heating for laser operation on the 1st-Stokes line we calculate the focal length of the thermal lens to be approximately 34 mm. However experimentally we see from the data in Fig. 7 for a resonator length of 24 mm that the 1st-Stokes power passes through a maximum at only 18 W pump power, suggesting that the thermal lens is much stronger ($f \sim 20$ mm) than the estimate based on pump and Raman heating alone. As we previously noted for cw Raman lasers based on discrete laser and Raman crystals [4] there appear to be additional thermal loading processes in play which are yet unidentified. These may include trace impurity absorption or excited-state absorption in the laser/Raman crystal (we note that the Nd:GdVO₄ crystal emits a strong blue fluorescence above Raman threshold).

If we further account for the backwards generated yellow light, assuming that 95% of the yellow output is absorbed in the Nd:GdVO₄ crystal we estimate the induced thermal lens to have focal length ~ 26 mm, approximately 30% stronger than for 1st-Stokes-only operation. Based on the data of Fig. 7 we estimate the thermal lens power for frequency-doubled operation is indeed $\sim 30\%$ stronger than for 1st-Stokes-only operation, suggesting that the source of unidentified additional heating is associated primarily with the Raman process alone.

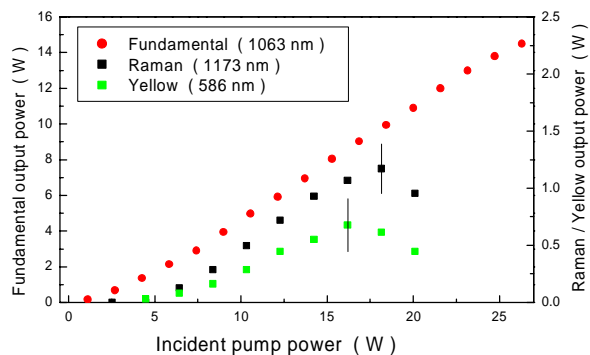


Fig. 7. Optimized fundamental, Raman and yellow output power as a function of incident pump power for a fixed physical cavity length of 24 mm.

Strategies to reduce the thermal load and hence the induced lens are currently being investigated and include; using higher purity crystals, redirecting the yellow light with an intracavity mirror and reducing the intracavity intensity through improved extraction of the Raman optical field. Alternatively by accommodating the thermal load into the resonator design, for example, using a convex input mirror to partially offset the thermal lens should improve the resonator stability and hence power extraction.

6. Conclusion

We have demonstrated what we believe is the first diode-pumped continuous-wave self-Raman Nd:GdVO₄ laser with 1st-Stokes output at 1173 nm and intracavity frequency-doubled output at 586.5 nm. A maximum cw power at 1173 nm of 2 W was obtained for diode pump powers of 22 W whilst maximum cw powers at 586 nm of 678 mW were obtained with 16.3 W pump. Infrared and yellow powers were limited by thermal lensing in the gain medium and parasitic oscillations of other neodymium transitions. In quasi-cw operation at 50% duty-cycle much higher maximum yellow output powers were obtained as the reduced thermal load allowed cavity stability to be maintained up to the maximum available pump power. In this case we obtained a maximum yellow power of 1.88 W with 25.7 W incident pump power. Increased Raman output powers are expected using a longer Nd:GdVO₄ crystal in order to achieve higher Raman gains whilst also accommodating the strong thermal lens, while increased yellow output powers may be obtained by incorporating an intracavity mirror to collect both the forward and backward propagating yellow emission. We anticipate that by managing the thermal loading and collecting all the generated yellow emission, cw yellow output powers greater than 3 W can be achieved at >10% diode-yellow conversion efficiency for diode-pump power no greater than 30 W.